Design and Application of Intelligent Inspection System for Automated Operation and Maintenance of Energy Meters

Zhang Xinrui *‡, Jin Xurong *, Cheng Zhiqiang *, Li Yunpeng *, Fan Bo *, Chen Xu *, Wang Xiangwei *, Wang Mingqiang *, ilhan GARIP **

C*+ Eng., State Grid Ningxia Marketing Service Center (State Grid Ningxia Metrology Center), China
** Department of Electrical and Electronics Engineering, Nisantasi University, Istanbul, Turkey

(Esmaeilzadeh786@hotmail.com, xurong125@gmail.com, zhiqiang462@gmail.com, yunpeng@hotmail.com, Bo2024@hotmail.com, xuedu@gmail.com, xiangwei@hotmail.com, mingqiang@hotmail.com, ilhangarip60@gmail.com)

‡Corresponding Author; Zhang Xinrui, Eng., State Grid Ningxia Marketing Service Center (State Grid Ningxia Metrology Center), China.

Received: 09.02.2024 Accepted: 06.03.2024

Abstract- To ensure the stable and efficient operation of maintenance activities, it is essential to continuously monitor and maintain the performance indicators of energy meters so that they remain within normal operational parameters. Based on the .NET MVC (Model–View–Controller in the Microsoft .NET framework) architecture and the command–query duty separation read–write separation design pattern, an electric energy meter automatic operation and maintenance platform is developed. According to the practical requirements of inspection systems used in electric energy meter operation and maintenance, several functional modules are integrated into the platform. These include the electric energy meter number identification module, the temperature infrared detection module, and the line detection module, enabling key tasks such as meter number reading, temperature measurement, and line monitoring. After applying the intelligent inspection system to the automated operation and maintenance process of electric energy meters, experimental results demonstrate effective performance. When the spacing from the first measurement point is 25 cm and 0 cm, the no-load voltage values are 0.633 V and 1.269 V, while the load voltage values are 0.579 V and 1.237 V based on regulator voltage variation. The results show that the success rate of electric energy meter fault inspection reaches 100%. The system demonstrates good stability, linearity, and reliability, confirming the effectiveness of the proposed intelligent inspection approach.

Keywords Electricity meter automation operation and maintenance, intelligent inspection system, meter number identification module, temperature infrared detection module, line inspection module.

1. Introduction

Energy meters are the medium of settlement between electricity users and power supply enterprises and are subject to key state regulation [1]. It serves as the basis for payment of electric energy, which is related to the production life and daily livelihood of the society. As an electric power metering apparatus with high application frequency, energy meters are widely used at the end of the electric power system to provide data reference for electric power measurement and power supply cost accounting [2-6]. This is because risk factors such as incorrect wiring, incorrectly set parameters, and interference with communication signals can lead to abnormalities in the energy meter, affecting the accuracy of the energy measurement and impeding the normal operation of the grid [7-9]. Therefore, the operation and maintenance of energy meter automation is carried out smoothly. The specific content of operation and maintenance work mainly includes on-site calibration, fault detection, periodic calibration, equipment inspection and maintenance, etc. [10-13]. Only when hidden faults or problems with the meters are detected in time can the calibration and repair of the equipment be done effectively, so that risks and even losses can be avoided to the greatest extent possible. In general, the operation and maintenance cycle of energy meters is fixed [14]. However, the actual working environment and external factors can easily result in large differences in calibration results within the same cycle. If the O&M cycle is set too short, it will add a lot of extra workloads. Operation and Maintenance (O&M) refers to the activities and processes involved in the operation, upkeep,

and management of various systems, facilities, or equipment to ensure their continued functionality, efficiency, and safety. Overall, effective operation and maintenance practices are essential for ensuring the reliability, efficiency, and safety of infrastructure, equipment, and systems across various industries and sectors. Therefore, it is significant to study an intelligent system for inspecting the automatic operation and maintenance status of energy meters. This can not only improve the operation and maintenance management level and efficiency, make the energy meter improve quality and efficiency, but also help to achieve sustainable development of power enterprises [15].

With the rapid rise of the major enterprises in various fields, high-tech science and technology was introduced in large numbers, intelligent inspection technology and operation and maintenance technology were popularized, and achieved good results in various industries. Like in the literature [16], an intelligent inspection tool is used to collect information on corrosion defects in the pipeline space and analyze the corrosion rate, failure pressure moments, etc., so that the time-dependent reliability of the pipeline can be assessed. The literature [17] designed a novel machine learning model to be applied in mobile and O&M maintenance systems for intelligent inspection of road conditions. Its inclusion in the committee machine intelligence system substantially increases the accuracy of road modeling and can predict more accurate road condition indices. In the literature [18], an intelligent inspection system for detecting defects on steel surfaces was architected based on a single-stage detector in combination with computer vision technology. The system is able to effectively deal with a variety of situations such as disturbing image backgrounds, easily confused defect types, highly variable defect sizes, and minor defects that are not easily detected. In the literature [19], a regional convolutional neural network infrared detection model is designed for the infrared devices of substation intelligent inspection robots. The basic features are clarified by observing the infrared images of various types of electronic devices. And fast area convolutional neural network target detection algorithm is invoked to improve the recognition accuracy of targets in images. In the literature [20], the path planning problem of multi-inspection robots is studied for large substation inspection in smart microgrids. By improving the bio-inspired neural network, the multi-robot is allowed to accurately complete single-area inspection, multi-area inspection, and all-area inspection with the support of a collaborative inspection system. The results achieved by O&M technology are mainly in industry, telecommunications, electric power, and public facilities management. For example: the literature [21] made an exploration of the O&M study of offshore wind turbines. It was found that offshore wind farms often use condition detection equipment to identify turbine faults and evaluate its performance. Based on previous O&M planning literature, the strengths and weaknesses of the wind industry and future trends in O&M technology are discussed. The literature [22] builds a telecommunication platform O&M system based on the integration of Apriori association rules to speed up the O&M collaboration and improve the informatization of the platform. According to the practice results, the built O&M system not only increases the tightness of sales-operations collaboration, but also increases the accuracy of risk prediction. The literature [23] architects visualization architecture for smart distribution grid situational awareness in terms of three situational awareness phases: detection, understanding, and prognosis, with a view to providing different insights in terms of related technologies, with respect to the need for high-quality operation and maintenance of smart distribution grids. The literature [24] enriches this standard for industry base classes using O&M semantics based on the data architecture for infrastructure project modeling. And through the open building information modeling process, the integration of O&M data is done in the building information model of road infrastructure. The currently achieved intelligent inspection technology and operation and maintenance technology achievements are separate, and there are few studies that effectively integrate the two technologies together, resulting in a gap in the integration of such technologies. This provides some ideas for the proposed research topic [25].

Intelligent inspection technology and operation and maintenance technology have their own advantages, and both have good prospects for development. Therefore, this paper tries to combine the two technologies and proposes the design of an intelligent inspection system with the goal of improving the level of automatic operation and maintenance of energy meters, and discusses its applicability. ASP.NET MVC is used as the basic framework structure of the core system to build the energy meter automation operation and maintenance platform under the command-query-duty-separation read-write separation design pattern. Gaussian difference pyramids are used to obtain multi-scale features of images in different spaces by Gaussian blurring and down sampling to build out the scale space. The gradient information contained in the key point feature vector is counted to generate a multi-dimensional feature vector, and the normalization process is expanded to complete image matching. Pre-process the matched energy meter images and correct the pre-processed energy meter images by using perspective transformation algorithm. Arrange and combine the recognition results to realize the reading of the energy meter number. Design an infrared detection module using an infrared detector with electronic scanning capability to monitor the temperature of the energy meter. Design a sensor device through electric field coupling to complete line detection without touching the energy meter. The purpose of this research project is to ensure the normal and stable operation of the energy meter and to complete the measurement tasks safely and accurately. At the same time, it provides good technical support to the operation and maintenance management of power supply enterprises' electric energy meters, guides the future development direction of electric energy metering devices, and dynamically innovates the operation and maintenance strategy of electric power equipment.

2. Design of Intelligent Inspection System for Automated Operation and Maintenance of Energy Meters

Build a meter automation operation and maintenance platform (electric meter), and utilize it as the foundation for developing an intelligent inspection system. According to the

actual utility that the inspection system needs to produce in the operation and maintenance of electric energy meters, add corresponding functional modules and intelligent algorithms to the operation and maintenance platform. By empowering the inspection system with the ability to realize the functions of meter number identification, temperature infrared detection, and line monitoring, the efficient work efficiency of operation and maintenance is ensured.

2.1. Automated Operation and Maintenance Platform for Power Meters

The core of the energy meter automation operation and maintenance platform is the web-site management system. The system needs to have various functions, such as accessing energy meter marketing data, interfacing with automated inspection line management system data, interfacing with mobile application external interface, presenting data management interface, etc. Therefore, ASP.NET MVC is used as the basic framework structure of the core system to build the energy meter automation operation and maintenance platform under the CQRS (Command Queries Responsibility Segregation) read-write separation design pattern. As shown in Figure 1. This O&M platform always contains five layers, which are data storage layer, data warehousing layer, service layer, business logic layer, infrastructure layer, and external interface layer.

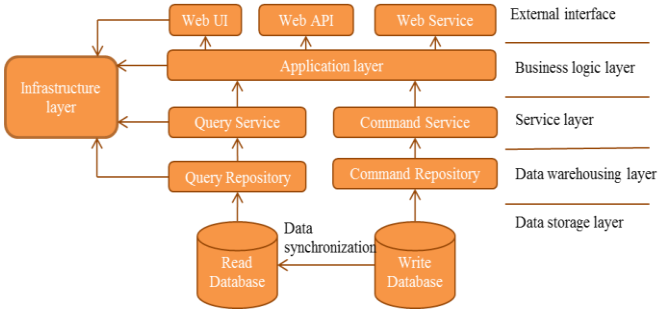

Fig 1. Schematic diagram of the electricity meter automation operation and maintenance platform.

The ASP.NET MVC structure is divided from the functional point of view to get three parts: the model layer, the view layer, and the controller layer. The role of the model layer is to interact with the model and database used and to handle the data logic contained in the application. The role of the view layer is to store the client interface files and present the client interface using the view and its rendering engine. The role of the controller layer is to integrate the model layer with the view layer to allow some of the functions of the business logic layer to operate and interact with the client and the web application. The data related to the business objects are processed in the model layer and the different processing results are presented in the view layer. Using the command-query-duty-separation read-write separation design pattern to reclassify the controller layer and the model layer, the business logic layer is separated from the data query/modification functions of the database, which reduces the amount of code in the business logic layer, improves code maintenance, and gives the code scalable properties. At the same time, the command-query-duty-separation read-write design pattern helps speed up the response speed of the operation and maintenance platform and strengthen the performance of the database server by separating the database layer.

2.2. Energy Meter Count Recognition Module

2.2.1 Image matching

Before matching the energy meter image, a scale space needs to be constructed. Suppose an energy meter two-dimensional bit image $I(x,y)$ is and the Gaussian function of scale variation is $Q(x,y,\sigma)$, then the corresponding scale space expression is shown as follows.

$$L(x,y,\sigma)=Q(x,y,\sigma)*I(x,y) \quad (1)$$

The $*$ in this equation represents the form of convolution operation. If the specification of the Gaussian template is $m\times n$ and the variance is σ^2, then the formula for the Gaussian function is shown below.

$$G(x,y)=\frac{1}{2\pi\sigma^2}e^{-\frac{(x-m/2)^2+(y-n/2)^2}{2\sigma^2}} \quad (2)$$

To solve the multi-scale feature differences of images in the scale space, a Gaussian difference pyramid is used to obtain the multi-scale features of images in different spaces by Gaussian blurring and downsampling to build the scale space. The initial image of the initial power meter is placed at the bottom of the pyramid, and after the downsampling process, the pyramid is made in a sequence state from bottom to top, and images are obtained. Assuming that the image specification $M\times N$ and the logarithm of the image dimension at the top of the pyramid is n, the number of images can be solved by the following equation.

$$n=\log_2\left[\min(M,N)\right]-tt\in\left[0,\log_2\left\{\min(M,N)\right\}\right] \quad (3)$$

In the constructed Gaussian differential pyramid scale space, the scale-invariant feature transformation algorithm is used to find the extreme points of the pyramid and compare them one by one. The extreme value obtained after comparing the intermediate detection points is the alternate key point in this scale space. A range is specified with the currently selected key point as the center of the circle, and the histogram is constructed using the gradient directions of all the sampled points in that range. The main direction of this key point is determined by the gradient direction of most of the sampled points and does not change in any way as the image changes. It is known that the corresponding value of this key point in the scale space is $L(x,y)$, the gradient is $m(x,y)$, and the gradient direction is $\theta(x,y)$. Then, the neighbouring pixel gradient of this key point and its direction can be determined by the following set of equations.

$$\begin{cases} m(x,y)=\sqrt{\left[L(x+1,y)-L(x-1,y)\right]^2+\left[L(x,y+1)-L(x,y-1)\right]^2} \\ \theta(x,y)=\arctan\dfrac{L(x,y+1)-L(x,y-1)}{L(x+1,y)-L(x-1,y)} \end{cases} \quad (4)$$

Combine the position, gradient and its direction of the key point to form the descriptor of the key point. Explicitly define the spatial region of the key point descriptor, and divide the neighbourhood into multiple square pixel blocks of the same size. Rotate the image according to the principal direction of the key points so that the principal direction is the same as the horizontal direction x. Suppose the coordinates of the key point before image rotation are (x, y) and the rotation angle is θ Then, the position of the coordinates of the key point after rotation is shown as follows.

$$\begin{pmatrix} x' \\ y' \end{pmatrix} = \begin{pmatrix} \cos\theta & -\sin\theta \\ \sin\theta & \cos\theta \end{pmatrix} \begin{pmatrix} x \\ y \end{pmatrix} \quad (5)$$

The key point neighborhood in the rotated image is divided into pixel blocks once more, the gradient information contained in the key point feature vector is counted, the multidimensional feature vector is generated, and the normalization process is expanded. Assuming that the descriptor of the key point is h_i, after normalization, the descriptor of this key point is expressed by the following equation.

$$L_i = \frac{h_i}{\sqrt{\sum_{i=1}^{128} h_i^2}} \; i = 1, 2, 3, \ldots, 128 \quad (6)$$

Based on the obtained image key points, image matching is completed.

2.2.2 Image recognition

The matched energy meter images were preprocessed. The processing means are grayscale, Gaussian filtering, adaptive threshold segmentation, and morphological processing (expansion and erosion). In order to avoid distortion of the image, the preprocessed energy meter image is corrected to be in a regular condition using a perspective transformation algorithm. Based on the principle of image to plane projection, the following 3D matrix is used for implementation, ensuring the flexibility of linear transformations and spatial translations.

$$\begin{bmatrix} X \\ Y \\ Z \end{bmatrix} = \begin{bmatrix} f_{11} & f_{12} & f_{13} \\ f_{21} & f_{22} & f_{23} \\ f_{31} & f_{32} & f_{33} \end{bmatrix} \quad (7)$$

Knowing a two-dimensional point and a three-dimensional point, the point transformation from two-dimensional to three-dimensional is realized by the following equation.

$$\begin{aligned} X &= f_{11} \times x + f_{12} \times y + f_{13} \\ Y &= f_{21} \times x + f_{22} \times y + f_{23} \\ Z &= f_{31} \times x + f_{32} \times y + f_{33} \end{aligned} \quad (8)$$

If you want to obtain the result of the conversion of a three-dimensional point (X, Y, Z) in another two-dimensional plane, obtaining the coordinates of a two-dimensional point consisting of horizontal coordinates x' and vertical coordinates y', the conversion can be done by the following two expressions.

$$x' = \frac{X}{Z} = \frac{f_{11} \times x + f_{12} \times y + f_{13}}{f_{31} \times x + f_{32} \times y + f_{33}} \quad (9)$$

$$y' = \frac{Y}{Z} = \frac{{}_{21} \times x + f_{22} \times y + f_{23}}{f_{31} \times x + f_{32} \times y + f_{33}} \quad (10)$$

The trained deep learning mobile net-yolo v3 algorithm is used to explicitly, detect the location in the energy meter image where the meter count can be read, and extract the meter count display region in it. If the region is I_{yx}, then x, y in it should satisfy the following inequality relation.

$$1 \le x \le Width\ of\ indication\ area \quad (11)$$

$$1 \le y \le Height\ of\ indication\ area \quad (12)$$

Assuming that the center point of the image Ic of the table number display section is $p(x_0, y_0)$, the upper and lower boundaries of the table number symbols, after being calibrated by the straight line l, yield the coordinates $p_1(x_1, y_1)$ and $p_2(x_2, y_2)$ of the two endpoints. from this, the formula for calculating the angle between the straight line and the horizontal direction can be deduced as follows.

$$\theta = \arctan\left(\frac{y_2 - y_1}{x_2 - x_1}\right) \quad (13)$$

Then the expression of the rotation matrix with the center point as the origin can be defined by the following equation.

$$\Gamma = \begin{pmatrix} \cos\theta & -\sin\theta \\ \sin\theta & \cos\theta \end{pmatrix} \quad (14)$$

The positive direction of the rotating energy meter using the rotation matrix in the above column is the horizontal direction, at this time, the image is Γ_c. The smallest external rectangle L_{ij} of the meter number display area is selected, so that the number of meter symbols in it is 1. Dividing this rectangle according to the positive direction, the following expression is obtained.

$$C_k = I_c^{'}\left[y_1 : y_m, x_1 + (k-1) \bullet w : x_1 + k \bullet w - 1\right] (1 \le k \le l) \quad (15)$$

Dividing the smallest external rectangle according to the vertical direction into n parts, the expression for the fractional reading part of the table number is given as follows.

$$D = I_c^{'}(y_M - h - 1 : y_M, x_1 : y_N) \quad (16)$$

The image of the read part of the table number (except for the decimal part) is used as an input item and input to the convolutional neural network model for recognition. The decimal part of the table number is recognized using the

correlation filter tracking algorithm. The two results obtained from the recognition are arranged and combined to achieve the reading of the energy meter. The principle of the correlation filter tracking algorithm is to train the correlation filter based on the correlation present in the signal processing and the extracted target features, and to filter the input image of the next frame. If the similarity between two signals is higher, the correlation value solved by the filter at that position is higher.

2.3 Energy meter temperature infrared detection module

The temperature of the energy meter is also one of the important monitoring indicators on the automated operation and maintenance platform. Therefore, an infrared detection module for energy meter temperature is designed using an infrared detector with electronic scanning function. The specific structure is shown in Figure 2. An optical system is first used to focus the infrared radiation of the energy meter within the array surface of the detector for imaging. The converted electrical signal is then linearly processed using amplification circuits, compensation circuits, and other devices. Through the image acquisition module that comes with the infrared thermal imaging equipment, a thermal image of the distribution of the external temperature of the energy meter is formed. Finally, the thermal image stored in the image store is displayed through various terminals.

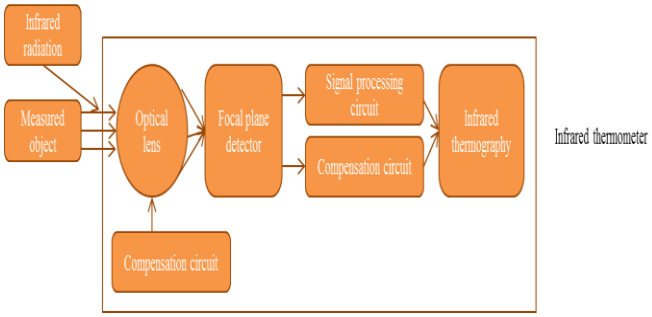

Fig 2. Schematic diagram of the structure of the infrared detection module for energy meter temperature.

The theoretical basis of the temperature infrared detection module of the energy meter is Planck's blackbody radiation law. Assuming that the absolute temperature and emissivity of the energy meter are T and $\varepsilon(\lambda)$, the wavelength and flux density of the spectral radiation are λ and $f(\lambda T)$, the operating wavelength of the thermal imaging camera is from λ_1 to λ_2, and its instantaneous field of view angle and total spectral response are ω and $R(\lambda)$, respectively, the signal amplitude of an imaging point of the energy meter under ideal conditions is calculated as shown below.

$$U_s \infty \frac{\omega b T^5}{\pi} \int_{\lambda_1}^{\lambda_2} f(\lambda T)\varepsilon(\lambda)\tau_\alpha(\lambda)R(\lambda)d\lambda \quad (17)$$

In the above equation, the atmospheric passage rate reaches and refers to the Boltzmann constant.

Based on the limited wavelength interval, the energy meter describes the grayscale value of each pixel with the voltage U' after amplifying and quantizing the signal amplitude when performing infrared thermal imaging. The expression form is shown below.

$$U' = kk_1\varepsilon F(T) \quad (18)$$

Within this equation, k and k_1 are two constant terms, the former only about the system gain and the latter only about the amplification of the thermal imaging device.

If the parameter ε always takes the value 1 and there is a functional relationship between the pixel grayscale U' and the temperature of the energy meter T. The blackbody imaging grayscale at the same temperature is described by the corresponding voltage value U, which is solved by the following equation. Based on the blackbody voltage-temperature curve, the relationship between the two is clarified and the corresponding temperature value is obtained.

$$U = \frac{U'}{\varepsilon} \quad (19)$$

The relative temperature difference judgment method is adopted as the basis for determining the heat generation of the energy meter to avoid miscalculation of fault defects and to reduce ineffective maintenance and repair workload. When the energy meter has the same physical properties, ambient temperature, load current and other conditions, and works in the same operation mode, assuming that the temperature rise and temperature value of the fever point are t_1 and T_1, and the temperature rise and temperature value of the normal relative point are t_2 and T_2, the difference between the temperature rise value of the two test points and the temperature rise value of the fever point is the relative temperature difference of the two test points. Can also be expressed in terms of the difference between the test point temperature value as a percentage of the difference between the normal relative point and the ambient temperature value T_0. The mathematical expression is shown below.

$$\Delta t = \frac{t_1 - t_2}{t_1} = \frac{T_1 - T_2}{T_1 - T_0} \quad (20)$$

2.4 Power Meter Line Detection Module

The process of automated operation and maintenance of energy meters is an important element in ensuring smooth and smooth line energization. Therefore, a sensor device is designed to obtain the differential component of the voltage value of the detection object relative to time, and the detection of the line can be done without touching the energy meter through the method of electric field coupling. The constructed equivalent model of the electric field coupled sensor is shown in Figure 3. In this detection module, the larger the voltage value of the line to be measured, the larger the integration of the measured value of the sensor. The integrator is introduced to prevent the positive correlation between the two from affecting the accurate measurement of the actual voltage value of the line.

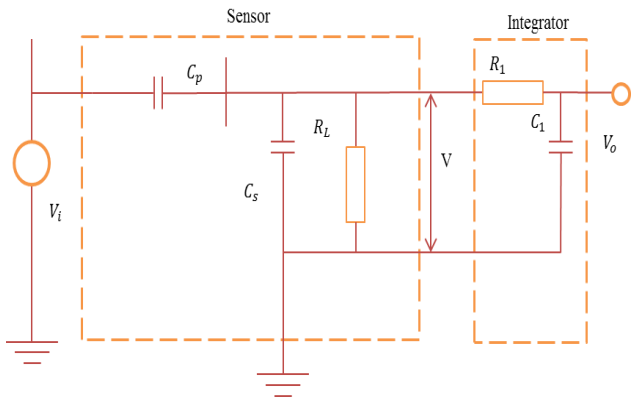

Fig 3. Schematic diagram of the equivalent model of the electric field coupled sensor.

Knowing that the equivalent potential of the detection line V_i and the sensor ground capacitance C_s, the coupling capacitance between the metal pole plate and the line is C_p, and the load impedance is R_L, the expression of the sensor transfer function in the equivalent model is shown as follows.

$$H_1(s)=\frac{V(s)}{V_i(s)}=\frac{sR_LC_p}{sR_L(C_p+C_s)}+1 \quad (21)$$

It is known that the capacitance and resistance of the integrator are R_1、C_I, and the output value of the integrator is V_o, then the expression of the integrator transfer function in the equivalent model is shown as follows.

$$H_2(s)=\frac{V(s)}{V(s)}=\frac{1}{sC_1R_1+1} \quad (22)$$

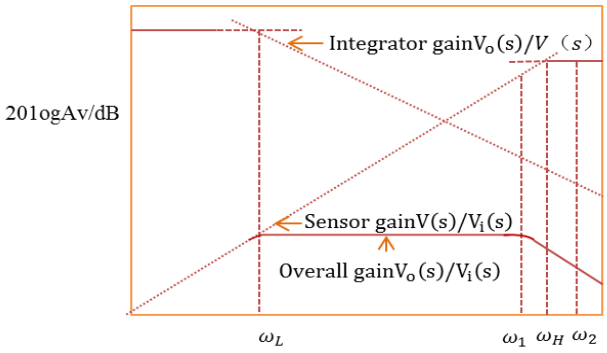

Fig 4. Amplitude and frequency diagram of the line detection module.

Based on the amplitude and frequency variations in the figure, it can be seen that the turn frequencies of the integrator and sensor are calculated by the following two equations, respectively.

$$\omega_L=\frac{1}{C_1R_1} \quad (23)$$

$$\omega_H=\frac{1}{R_L(C_p+C_s)} \quad (24)$$

When $R_L(C_p+C_s)\gg 1$ holds, the approximation of the sensor gain is obtained using the following equation.

$$\frac{V(s)}{V_i(s)}=\frac{C_p}{C_p+C_s} \quad (25)$$

If $R_L(C_p+C_s)\ll 1$ holds, the approximation of the sensor gain at this time is obtained by combining the amplitude-frequency curve using the following equation.

$$\frac{V(s)}{V_i(s)}=sR_LC_p \quad (26)$$

The current operation of the sensor is differential, which means that only the integrator and the sensor work together to make the voltage relationship between the input and output linear and thus obtain a stable gain. The current is measured by a relatively mature Hall sensor to meet the design requirements of the detection module for low cost and high accuracy.

3. Application of Intelligent Inspection System for Automated Operation and Maintenance of Power Meters

In order to ensure the orderly development of energy meter operation and maintenance work, the experimental session was tested from two aspects of energy meter line inspection and fault inspection respectively.

3.1 Energy Meter Line Inspection Effect Discussion

In order to test the stability and linearity of the intelligent inspection system, two test conditions are set up for no-load and load respectively. Compare the voltage at each position on the line of the energy meter under different conditions with the voltage at the fixed point when the contact regulator outputs different voltages. The contact regulator was used to ensure that the energized voltage of a line was always 220V, and the orientation of the sensing electrode on the line was changed to monitor the no-load voltage value and the load voltage value at locations with the first measurement point spacing of 0cm, 5cm, 10cm, 15cm, 20cm, and 25cm, respectively. As shown in Figure 5(a). Where the load voltage value is the experimental data obtained by connecting the contactor coil to the contact regulator as a load. Figure 5 (b) shows the no-load voltage value and load voltage value when the inductor electrode on the line is 20cm away from the first measurement point, and the voltage output of the contact regulator is 0V, 50V, 100V, 150V, 200V, 250V, respectively. The load conditions are the same as the load conditions set in the stability testing test.

By comparing Figure 5(a): the no-load voltage value increases as the spacing from the first measurement point decreases, but the increase is very small. When the distance from the first measurement point is 25 cm, the no-load voltage value is 1.245 V. When the distance is 20 cm, the no-load voltage value is 1.246 V. When the distance is shortened from 15 cm to 0 cm, the no-load voltage value increases from 1.249 V to 1.261 V. The load voltage value, however, does not show a more significant regular characteristic with the distance of the measurement point, and is always in the range of 1.1415V

up and down in a small range. These two sets of experimental data show that the constructed intelligent inspection system can obtain a relatively stable measurement result under the joint collaboration and mutual cooperation of the platform and each functional module, regardless of the no-load condition or load condition, and regardless of the distance from the first measurement point. Although some slight voltage fluctuations are generated from time to time, they do not affect the stability of voltage measurement in any way.

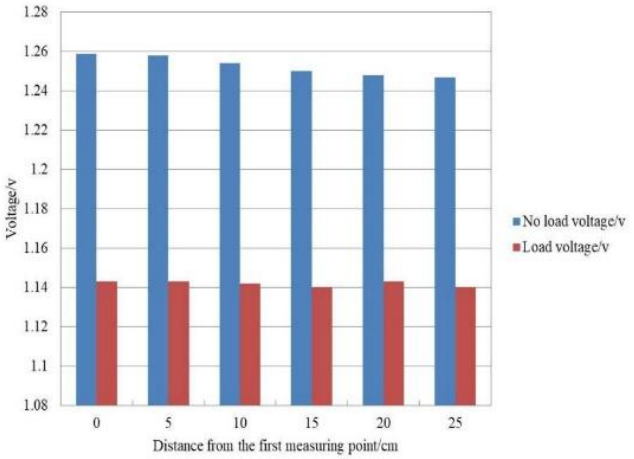

(a) Voltage at different locations of the line

By comparing Figure 5 (b): the two conditions of the voltage value with the contact regulator output voltage rises and becomes larger, and the rise shows a certain linear trend. When the regulator output voltage is 0V, the no-load voltage and load voltage values are 0.633V and 0.579V. When the voltage output 50V, the corresponding voltage values of the two conditions are 0.781V and 0.739V. When the output voltage is 100V and 150V, the voltage values are 0.908V and 0.896V, 1.045V and 1.044V. When the measured voltage values are 1.183V, 1.138V, 1.269Vand 1.237V.when the voltage output is 200V and 250V respectively.

The introduction of the integrator in the line detection module of the energy meter effectively avoids the influence of the relationship between the line voltage value to be measured and the integrated amount of the measured value of the sensor on the accurate measurement of the voltage value. So the designed line detection module can still effectively collect voltage information when the voltage output of the contact regulator is 0V. Similar to the stability test results, despite several voltage fluctuations, it still does not affect the overall detection effect of the intelligent inspection system on the energy meter line. In summary, the designed intelligent inspection system can guarantee the monitoring of different conditions under different conditions in the process of automatic operation and maintenance of energy meters. The reliability of the system has significant advantages and can give effective reference basis for the line of electric energy meter, providing strong technical support for the later line breakage and breakage fault investigation.

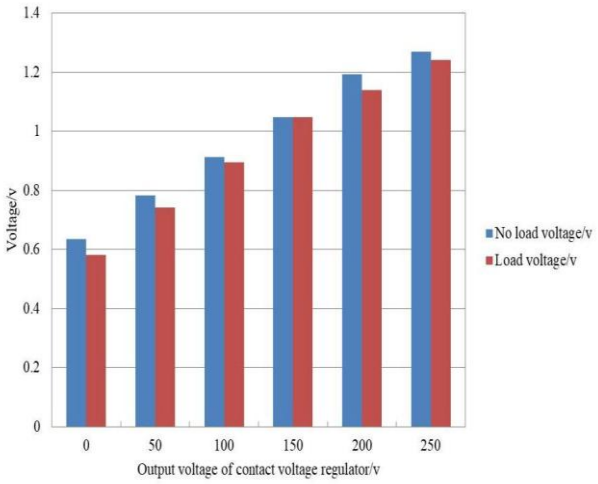

(b) Measurement results of different voltage values

Fig 5. Schematic diagrams of power meter line stability and linearity evaluation.

3.2 Electricity Meter Typical Fault Patrol Effect Discussion

From the intelligent inspection system in the electric energy meter automation operation and maintenance for a period of ten months of trial operation stage, the more common electric energy meter fault in the operation and maintenance process is classified into five types, namely: the electric energy meter overall device fault, voltage secondary circuit fault, line connection fault, error overrun fault and electric energy meter fault. The verification purpose of this experiment is to test the practical application effect of the inspection system, to see whether the intelligent inspection system can accurately determine the type of fault that has a greater probability of occurrence when the electric energy meter works, and to verify the accuracy and effectiveness of the inspection system. The inspection results of the intelligent system on the typical faults of four energy meters are shown in Figure 6.

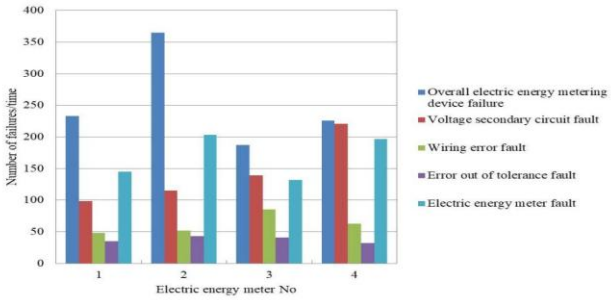

Fig 6. Typical fault inspection of energy meters in operation and maintenance.

According to the inspection data results of the intelligent system on the electric energy meter faults, it can be seen that the occurrences of the overall device faults of the four electric energy meters are 232 times, 367 times, 187 times and 226 times respectively. The occurrences of voltage secondary circuit faults are 98 times, 115 times, 140 times and 221 times respectively. The numbers of occurrences of line connection faults were 47, 54, 85, and 63, respectively. The occurrences of error overrun faults were 36, 41, 41, and 32 times

respectively. The occurrences of power meter faults are 144, 205, 132 and 197 times respectively. The number of times of all kinds of typical faults diagnosed by the above intelligent inspection system is consistent with the actual number of these kinds of faults of the electric energy meter, and the success rate of the intelligent inspection system's inspection of electric energy meter faults is as high as 100%, and there is no error detection or omission. The experimental data of this link fully verifies the rationality and feasibility of the intelligent inspection system.

4. Conclusion

Energy meter operation and maintenance is an important part of the grid statement cycle. Ensuring that energy meters are always in a healthy working condition is a key element of O&M. In order to ensure that the electric energy meter meets the requirements of normal and smooth operation, the article takes the automatic operation and maintenance of electric energy meter as the research object, builds the automatic operation and maintenance platform of electric energy meter, and uses it as the basis for the construction of intelligent inspection system. According to the utility existing in the operation and maintenance of the inspection system, the corresponding functional modules such as the number of energy meters identification and intelligent algorithms are added to the operation and maintenance platform to complete the system design. The following conclusions are summarized based on practical applications.

(1) The no-load voltage value increases as the distance from the first measurement point decreases. While the load voltage value does not show a more significant regular characteristic, always floating in a small range above and below 1.1415V. The constructed intelligent inspection system is able to obtain a relatively stable measurement result regardless of no-load conditions or load conditions, and regardless of the distance from the first measurement point.

(2) The no-load voltage and load voltage values are larger as the contact regulator output voltage rises, and the rise shows a certain linear trend. When the regulator output voltage is 0V, the no-load voltage and load voltage values are 0.633V and 0.579V respectively. The measured voltage values are 1.269V and 1.237V when the voltages are output at 250V respectively. Intelligent inspection system is superior to the overall detection effect of the energy meter line.

(3) The above intelligent inspection system diagnoses the occurrence of various types of typical faults to be consistent with the actual occurrence of these kinds of faults of the energy meter, and the success rate of the intelligent inspection system's inspection of energy meter faults is as high as 100%. The reasonableness and feasibility of the intelligent inspection system are fully verified.

Author Contributions

Zhang Xinru was responsible for the conceptualization, validation, resources, data curation, software development, and project administration. Jin Xurong, Cheng Zhiqiang, Li Yunpeng, Fan Bo, Chen Xu, Wang Xiangwei, Wang Mingqiang and ilhan GARIP jointly contributed to the methodology, formal analysis, investigation, original draft preparation, review and editing, visualization, supervision, and funding acquisition. All authors have read and agreed to the published version of the manuscript.

Conflict of Interest

The author(s) declared no potential conflicts of interest with respect to the research, authorship, and/or publication of this article.

References

[1] L. Peng, J. Li, J. Zhao, J. Z. Jingming, D. Sanlei, K. Zhengmin, and D. Li, “Automatic verification flow shop scheduling of electric energy meters based on an improved Q-learning algorithm,” Energies, vol. 15, p. 1626, 2022.

[2] S. Yljon, M. B. Steven, M. Christian, and G. S. Brian, “Power quality measurement and active harmonic power in 25 kV 50 Hz AC railway systems,” Energies, vol. 13, p. 5698, 2020.

[3] D. Yaping, W. Lu, J. Hao, Z. Xiaohui, and T. Xiangqian, “A deep learning method based on bidirectional WaveNet for voltage sag state estimation via limited monitors in power system,” Energies, vol. 15, p. 2273, 2022.

[4] L. Hao, Q. Ying, L. Longxiang, and Z. Baosen, “Power system transition with multiple flexibility resources: A data-driven approach,” Sustainability, vol. 14, p. 2656, 2022.

[5] M. Toledo-Orozco, C. Arias-Marin, C. Alvarez-Bel, and D. Morales-Jadan, “Innovative methodology to identify errors in electric energy measurement systems in power utilities,” Energies, vol. 14, p. 958, 2021.

[6] A. Koch, L. Nicoletti, T. Herrmann, and M. Lienkamp, “Implementation and analyses of an eco-driving algorithm for different battery electric powertrain topologies based on a split loss integration approach,” Energies, vol. 15, p. 5396, 2022.

[7] L. Meegahapola, A. Sguarezi, J. S. Bryant, M. Gu, E. R. Conde, and R. B. A. Cunha, “Power system stability with power-electronic converter interfaced renewable power generation: Present issues and future trends,” Energies, vol. 13, p. 5396, 2020.

[8] A. Nakhaei and F. Soltani, “Modelling and optimisation in the design of pipeline network systems using ant colony optimisation algorithm (ACO),” SRPH J. Interdiscip. Stud., vol. 3, pp. 1–17, 2021.

[9] X. Xu, L. Peng, Z. Ji, S. Zheng, Z. Tian, and S. Geng, “Research on substation project cost prediction based on sparrow search algorithm optimized BP neural network,” Sustainability, vol. 13, p. 13746, 2021.

[10] S. Khankalantary, S. Ranjbaran, and H. Mohammadkhani, “Simultaneous compensation of systematic errors of a low-cost MEMS triaxial

accelerometer and its temperature dependency without accurate laboratory equipment," Sensor Rev., vol. 41, pp. 208–215, 2021.

[11] R. U. Harvitkar and A. Joshi, "Iatrogenic bladder perforation post laparoscopic totally extraperitoneal inguinal hernia repair: Troubleshooting with laparoscopic approach," J. Minim. Access Surg., vol. 17, pp. 584–585, 2021.

[12] C. Kalogirou, M. Schwinger, A. Kocot, and H. Riedmiller, "Troubleshooting of failed continence mechanisms in the ileocecal pouch: Operative technique and long-term results of the intussuscepted ileal nipple valve," Int. J. Urol., vol. 28, pp. 1105–1111, 2021.

[13] S. P. Mirfasihi, S. Ghazali, and S. Baradaran Shokouhi, "Designing and implementing of real-time intelligent system with the ability to identify and classify different topics in autonomous vehicle," SRPH J. Interdiscip. Stud., vol. 4, pp. 1–7, 2022.

[14] H. Sadler, "R2C SDMLC: Enterprise release risk-centric systems development and maintenance life cycle," Softw. Qual. J., vol. 28, pp. 1755–1787, 2022.

[15] K. Chen, R. J. Mahfoud, Y. Sun, D. Nan, K. Wang, H. H. Alhelou, and P. Siano, "Defect texts mining of secondary device in smart substation with GloVe and attention-based bidirectional LSTM," Energies, vol. 13, p. 4522, 2020.

[16] Z. Djamel, B. Omar, Z. Hafsi, and M. B. Djukic, "Probabilistic analysis of corroded pipeline under localized corrosion defects based on the intelligent inspection tool," Eng. Fail. Anal., vol. 115, p. 104683, 2020.

[17] M. Rahimi Shahid, "Evaluation of multivariable regression in predicting rock slake durability index," SJFST, vol. 4, pp. 1–20, 2022.

[18] T. Lei, F. Lv, J. Liu, L. Zhang, and T. Zhou, "Research on fault detection algorithm of electrical equipment based on neural network," Math. Probl. Eng., Art. no. 9015796, pp. 1–10, 2022.

[19] N. Chen and Y. Wang, "Design and collaborative operation of multimobile inspection robots in smart microgrids," Complexity, vol. 2021, pp. 1–11, 2021.

[20] G. Rinaldi, P. R. Thies, and L. Johanning, "Current status and future trends in the operation and maintenance of offshore wind turbines: A review," Energies, vol. 14, p. 2484, 2021.

[21] C. Li, L. Liu, J. Zhao, and Y. Liu, "An experiment to design an operation and maintenance system integrating Apriori association rules for a telecom platform," Wirel. Commun. Mob. Comput., Art. no. 1185584, pp. 1–28, 2021.

[22] L. Ge, Y. Li, Y. Li, J. Yan, and Y. Sun, "Smart distribution network situation awareness for high-quality operation and maintenance: A brief review," Energies, vol. 15, p. 828, 2022.

[23] S. Ait-Lamallam, R. Yaagoubi, I. Sebari, and O. Doukari, "Extending the IFC standard to enable road operation and maintenance management through openBIM," ISPRS Int. J. Geo-Inf., vol. 10, p. 496, 2021.

[24] M. Kalantari, "Optimal design and scheduling of active distribution network with penetration of PV/wind/BESS energy systems considering the load side management," SJIS, vol. 3, pp. 1–13, 2021.

[25] M. Yargholi, "System level simulation of energy-detection based UWB receivers," SJIS, vol. 2, pp. 10–14, 2020.